

Partially Hydrolyzed Trimethylaluminum (PHT) as Heterogeneous Cocatalyst for the Polymerization of Olefins with Metallocene Complexes

ALEXANDER KÖPPL,¹ HELMUT G. ALT,¹ M. DEAN PHILLIPS²

¹ Laboratorium für Anorganische Chemie, Universität Bayreuth, D-95440 Bayreuth, Germany

² Phillips Petroleum Company, Research and Development Center, 74004 Bartlesville, Oklahoma

Received 20 December 1999; accepted 6 July 2000

ABSTRACT: A method for the preparation of a novel heterogeneous cocatalyst, partially hydrolyzed trimethylaluminum (PHT), has been developed and optimized for ethylene polymerization reactions. It is possible to generate PHT on nearly any support without much loss of catalyst activity. The carrier material can be SiO₂, AlF₃, B₂O₃, starch, cellulose, active carbon, polyethylene, polypropylene, polystyrene, etc. This new type of partially hydrolyzed trimethylaluminum (PHT) is synthesized by reacting such a carrier material with trimethylaluminum (TMA) in toluene to block all surface Lewis basic centers that could poison a cationic metallocene polymerization center. The subsequent addition of a calculated amount of water gives a heterogeneous PHT that is different from the common methylalumoxane (MAO). Various PHT cocatalysts were studied by ¹³C and ²⁷Al MAS NMR, scanning electron microscopy (SEM), and infrared spectroscopy (IR), and compared with solid MAO. Surface areas and porosities were determined according to the BET method. © 2001 John Wiley & Sons, Inc. *J Appl Polym Sci* 80: 454–466, 2001

Key words: supported methylaluminoxane; olefin polymerization; metallocene catalysts; PHT

INTRODUCTION

In the 1950s, Ziegler^{1,2} and Natta^{3–5} discovered that titanium halides, in combination with aluminum alkyls, give good catalysts for the polymerization of olefins, especially for the production of linear polyethylenes and polypropylenes. Sinn and Kaminsky^{6–8} found that the combination of zirconocene dichloride and MAO also formed a very active catalyst system for the polymerization of olefins. Until now, however, the high activities

were only achieved under homogeneous polymerization conditions with very high aluminum/metal molar ratios. In homogeneous polymerizations, the polymer formed (fluff) has a low bulk density, and consists of finely divided particles. These fluff characteristics are undesirable. By making the catalyst heterogeneous using appropriate carriers and support techniques, it is possible to control the morphology of the fluff, to increase the bulk densities and to eliminate the precipitation of the resin on internal reactor surfaces (fouling).

One method of forming heterogeneous metallocene/MAO catalysts is to attach the MAO to the surface of a silica gel.^{9–15} The MAO supported cocatalyst is formed directly by the reaction of

Correspondence to: H. G. Alt.

Contract grant sponsor: Phillips Petroleum Company.

Journal of Applied Polymer Science, Vol. 80, 454–466 (2001)
© 2001 John Wiley & Sons, Inc.

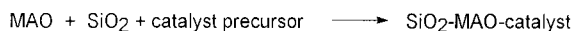


Figure 1 Synthesis of a heterogeneous catalyst with MAO as cocatalyst and silica as support.

MAO with functional groups on the silica gel surface.¹⁴ The disadvantage of this method is that it is often very difficult to attach all the aluminoxane onto the carrier material.

A significantly more effective procedure^{9–13} uses a nondehydrated silica gel that has been reacted in an inert solvent with trimethylaluminum (TMA). The water (8 wt %) absorbed on the silica reacts with the TMA to form MAO. In these methods, the hydrous silica gel is added in portions to a TMA hydrocarbon solution, whereby MAO is formed on the silica gel surface or in the silica gel pores. During the reaction there is always a local excess of water compared to the alkylaluminum component. Thus, some of the TMA forms aluminum oxide instead of MAO. These oxides cannot function as cocatalysts.

Commonly used carrier materials with high surface areas include, for example, silica gels or aluminas.¹⁶ However, these carrier materials exhibit one decisive disadvantage: they possess basic Lewis functional groups on their surface that react in a Lewis acid-base interaction with potential cationic polymerization centers (strong Lewis acids). This accounts for, at least in part, the extreme activity loss of the heterogenized catalyst systems compared to the homogeneous systems. If all the basic Lewis functional groups are first reacted with a strong Lewis acid, as for example TMA, the interaction of the cationic polymerization centers with the basic Lewis sites is prevented and productivities should be increased. Once the TMA has been attached to the silica, water can then be added to produce the methylalumoxane which serves as an effective cocatalyst for many olefin polymerization reactions.

We report here a novel method for the preparation of a heterogeneous form of partially hydrolyzed trimethylaluminum (PHT).

RESULTS AND DISCUSSION

According to the comments made above, various catalyst systems with different carrier materials

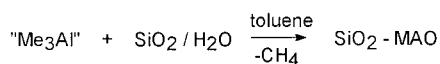


Figure 2 Synthesis of silica gel supported MAO.

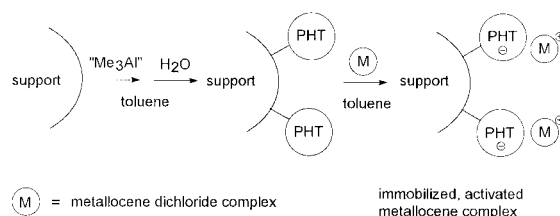
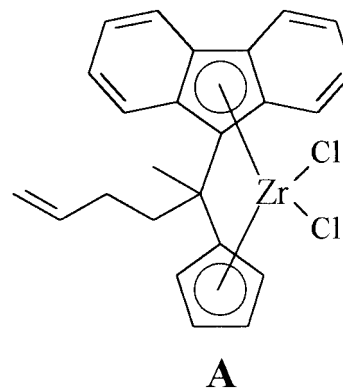


Figure 3 Synthesis of a heterogeneous metallocene catalyst with immobilized PHT.

were synthesized, as shown in Figure 3. Compared to previously known procedures, the key difference lies in the order of addition of water required for the synthesis of methylalumoxane. With this procedure we succeeded in completely immobilizing PHT on both polar carriers, such as silica and alumina, as well as on nonpolar carriers, such as activated carbon and polyethylene. The carrier materials used and the corresponding catalysts formed are listed in Table I. 2-(9-Fluorenylidene-1-cyclopentadienylidene)-hex-5-enylidene zirconium dichloride (A) was used as catalyst precursor.



²⁷Al MAS NMR Spectroscopy

The ²⁷Al NMR spectra of solid SiO₂-PHT 2 and starch-PHT 10 are significantly different from the spectrum of solid MAO. The solvent-free MAO shows three very broad, overlapping signals at 5, 33, and 65 ppm. The signals are related to various aluminum species of the fluctuating oligomeric species observed in solution. The spectrum is consistent with an amorphous MAO structure. The spherical charge distribution induces an electric field gradient on the nucleus that results in an increased signal width, especially for quadrupole nuclei, like ²⁷Al. The starch-PHT 10 cocatalyst system also has a rather broad signal around 20

Table I Properties of Various PHT Cocatalysts with 2-(9-Fluorenylidene-1-cyclopentadienyldiene)-hex-5-enylidenezirconium Dichloride as Catalyst Precursor

Catalyst Number	Support	Immobilization	Activity (kg PE/g Zr · h) ^a	M_n ^b (kg/mol)	T_m^1, T_m^2 (°C)	$\Delta H_m^1, \Delta H_m^2$ (J/g)	α (%)	Al : O
1	SiO ₂ ^c	+	125	113	—	—	—	1.44
2	SiO ₂	+	518	350	139.1	133.9	45.9	1.44
3	SiO ₂ · xH ₂ O	+	61	360	138.7	137.8	47.2	1.44
4	MgCl ₂	+	10	480	103.0, 137.5	2.86, 136.4	46.8	1.44
5	AlF ₃	+	296	300	136.9	142.7	48.9	1.44
6	B ₂ O ₃	+	166	281	142.3	137.8	47.2	1.44
7	B(OH) ₃	— ^d	—	—	—	—	—	—
8	Al ₂ O ₃	+	212	260	138.5	132.2	45.3	1.44
9	mol.sieves	+	163	295	138.5	132.2	45.3	1.44
10	starch	+	238	294	136.4	137.0	47.0	1.52
11	flour	+	220	305	135.2	133.87	45.9	1.52
12	cellulose	+	295	290	137.2	131.8	45.2	1.52
13	tylose [®]	+	160	255	95.2, 137.3	6.4, 134.3	46.0	1.44
14	aktive carbon	+	297	280	137.7	130.3	44.7	1.44
15	PE	+	280	215	138.2	146.4	50.2	1.44
16	PP	+	278	264	135.3	154.2	52.9	1.44
17	PS	+	190	240	137.0	130.3	44.7	1.44

^a Polymerization conditions for ethylene polymerization: 10.0 bar ethylene pressure, 500 mL pentane, 1.0 mL TIBA (1.6 M in *n*-hexane), 70°C, heterogeneous reaction, Al : Zr = 260 : 1, Al : O = 36%.

^b The molecular weight of polyethylene was determined by viscosimetry.

^c The silica was treated with the necessary amount of water before it was reacted with TMA.

^d Decomposes violently upon drying.

ppm, but not as broad as the signal for solid MAO. This indicates that the environment around Al is different. The ²⁷Al MAS NMR spectrum of the silica gel–PHT 2 system, however, is very different, and quite surprising. There is only one narrow signal at 2 ppm with a half-width of 53 Hz besides the spinning side bands (ssb). The chemical shift of this signal is characteristic of symmetrically coordinated, octahedral aluminum compounds.¹⁷ Therefore, MAO on silica gel 2 exhibits a defined, probably at least a partially crystalline structure, that has not been previously observed for MAO structures. Underneath the main signal, in the region between –20 and –40 ppm, there is a broad signal that indicates a small portion of an unsymmetrical aluminum environment.

¹³C MAS NMR Spectroscopy

The characterization of SiO₂–PHT 2 and starch–PHT 10 using ¹³C MAS NMR spectroscopy does not show significant differences in the chemical shift of the aluminum bonded carbon atoms (–10

ppm). In addition to the methyl region, a smaller signal is observed at approx. 51 ppm. Similar observations have already been published.¹⁸ This signal at $\delta = 51$ ppm is attributed to a carbon atom of a methoxy group indicating that a partial oxidation of an Al–Me bond to an Al–O–Me group has probably taken place. Despite strict exclusion of oxygen during the preparation of the samples, the NMR spectra of silica gel–PHT 2 (a) and starch–PHT 10 (b) have a clear signal at 51 ppm.

Scanning Electron Microscopy (SEM)

The pure, untreated carrier materials were characterized using SEM analyses to determine changes on the carrier surface due to synthesis of the catalyst system. The recordings were selected so that the most representative section was viewed. The materials analyzed were silica gel (a), starch (b), and aluminum trifluoride (c). Figure 6 exhibits the corresponding recordings at three different magnifications. The differences in the macroscopic structure of compounds a, b, and c are well pronounced. While silica gel has an

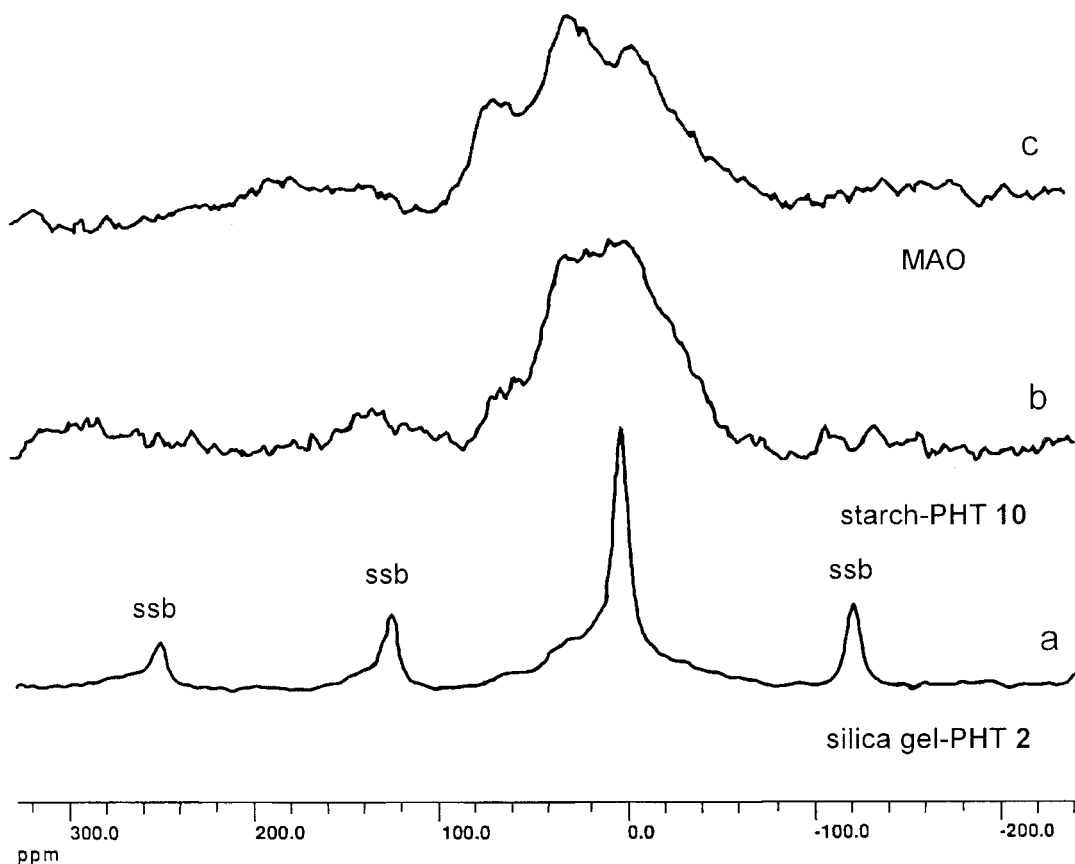


Figure 4 Solid state ^{27}Al -MAS-NMR spectra of (a) silica gel-PHT 2, (b) starch-PHT 10, and (c) solid MAO (ssb = "spinning side-band").

almost uniform particle size ($\phi = 20\text{--}70\ \mu\text{m}$), a spherical shape and a smooth surface, starch has an irregular distribution of the particle sizes ($\phi = 10\text{--}150\ \mu\text{m}$) with a highly rugged surface. Aluminum trifluoride appears as a microcrystalline material with a very small average particle size ($\phi = 5$ and $20\ \mu\text{m}$) and defined, plane surface (Fig. 6).

Regardless of the carrier material, the particle size after supporting the aluminoxane differs only slightly from that of the pure carrier material. Only silica gel-PHT 2 [Fig. 7(a)] exhibits a significant increase in the maximum particle size ($130\ \mu\text{m}$). This is caused by the agglomeration of individual particles with aluminoxane acting as a "molecular glue." In addition, multiple broken, semispherical silica gel particles are observed. This proves that the TMA is penetrating into the individual silica gel particles and causing the particles to burst due to methane gas evolution and to the formation of aluminoxane upon introducing water. The silica gel surface is completely covered with aluminoxane particles, and larger hollow

spaces are observed in the aluminoxane structures. The aluminoxane on the silica surface seems to consist of a conglomeration of individual spherical particles with an average particle size of about $400\ \text{nm}$.

In the case of the starch-PHT 10 cocatalyst [Fig. 7(b)], a slightly different picture emerges. At constant particle size between 10 and $200\ \mu\text{m}$, the surface covered with aluminoxane does not exhibit any larger gaps. A rather uniform distribution of spherical aluminoxane particles with an average particle size of $240\ \text{nm}$ is found. This size is clearly below the particle size found for silica gel-PHT 2. The uniform arrangement of the aluminoxane particles is a result of the large number of covalent bonding possibilities between the carrier (hydroxyl groups) and aluminoxane, which serves as a template for the formation of aluminoxanes.

Aluminum trifluoride-PHT 5 is again different. At best, a coordination bond can form between the fluorine atoms of the carrier material and the aluminum centers in the aluminoxane.

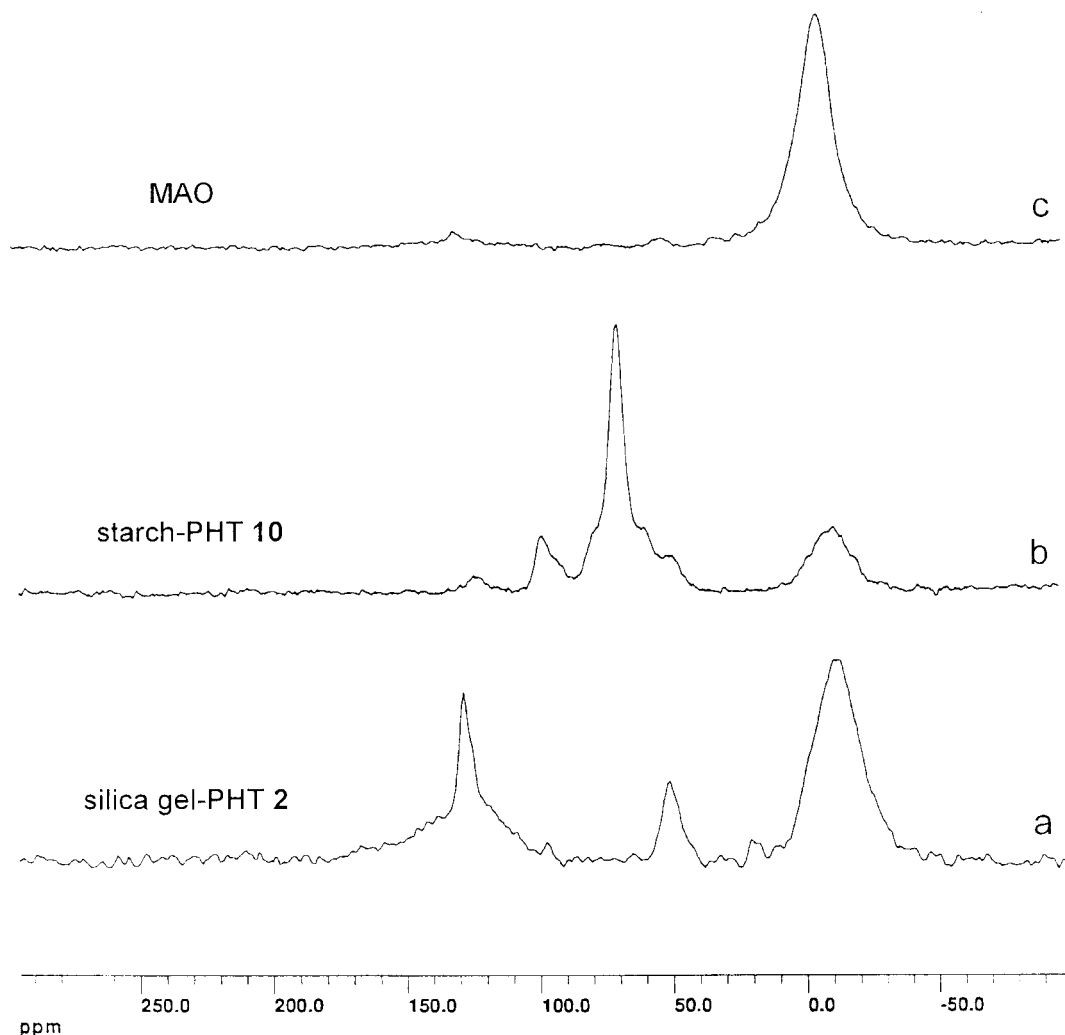


Figure 5 ^{13}C -MAS-NMR spectra of (a) silica gel-PHT 2, (b) starch-PHT 10, and (c) solid MAO.

Figure 7(c) shows that the aluminoxane particles are preferably located in the corners of two touching crystal planes. This observation leads to the hypothesis that the carrier material used is effective in providing nucleation centers for the aluminoxane particles. The average size of the irregularly shaped aluminoxane particles is around 300 nm, which is intermediate between the values for silica gel-PHT 2 and starch-PHT 10.

A special SEM sample preparation technique provides information on the "inside life" of a cocatalyst particle: in this case, the sample embedded in epoxy resin is stepwise polished off and covered with a thin layer of carbon in a vacuo evaporator. Suitable particles are identified using SEM and subsequently analyzed using X-ray analysis.

The silica gel-PHT 2 system with the standard catalyst precursor [9-fluorenylidene-1-cyclopentadienyldiene]-2-hex-5-enylidene zirconium dichloride (A)¹⁹ was investigated using this sample preparation technique. The corresponding recordings are summarized in Figure 8.

Picture 1 in Figure 8 (8-1) presents the SEM recording of a cross-section through several different particles. Particle c is unambiguously identified as a fragment of a spherical silica gel particle that resulted from the fracturing of a spherical particle due to formation of aluminoxane in the pore system of the silica gel. Particle b is characteristic of an intact silica gel particle. It has a slightly thicker aluminum layer (Picture 8-2) on its surface. More aluminum is found inside the particle, however, in lower concentration. The el-

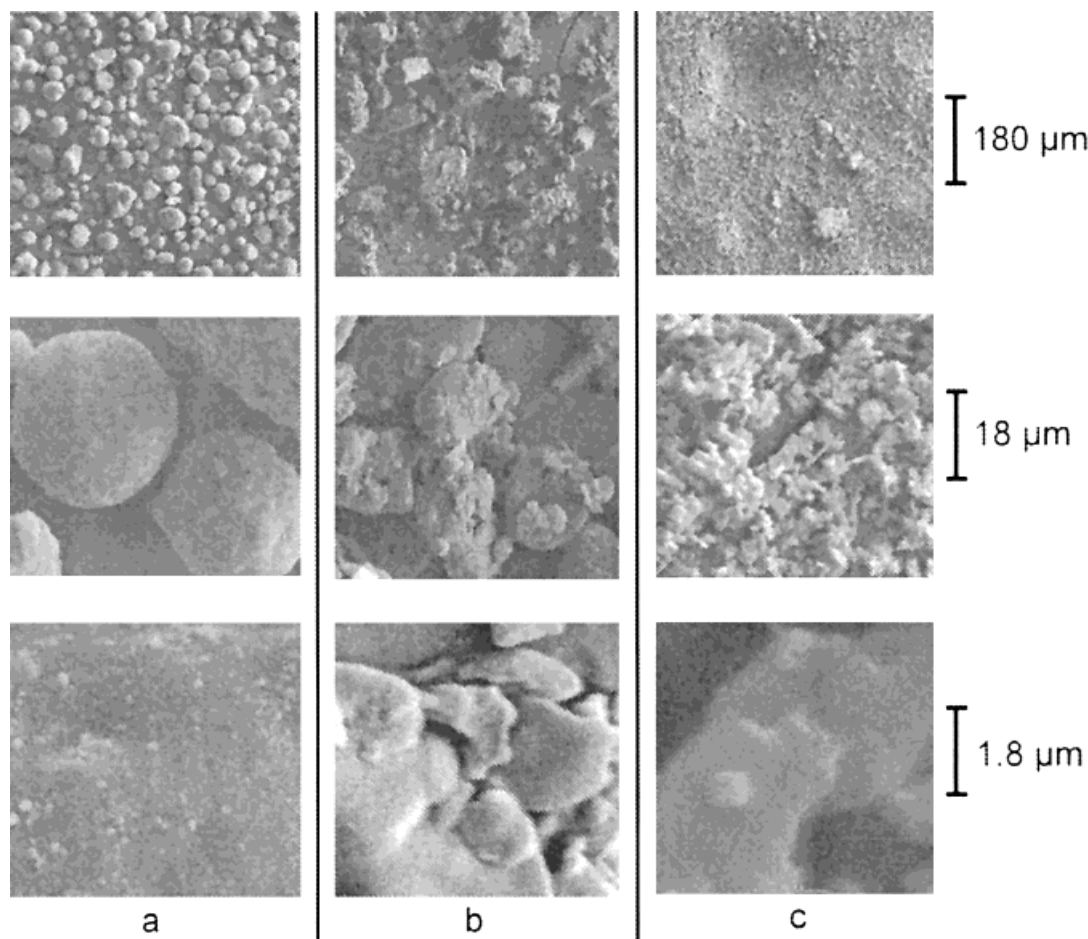


Figure 6 SEM-recordings of (a) silica gel, (b) starch, and (c) aluminumtrifluoride.

elements zirconium (8-3) and chlorine (8-6) are also detected in the silica gel particle, i.e., the pore system is still intact after supporting aluminoxane allowing penetration of the catalyst particles. Silicon is not found in particle a, and the zirconium and chlorine concentration are especially high. This indicates that the aluminoxane is not supported on the surface but rather condensed onto already supported aluminoxane structures. Due to the better porous structure of these aluminoxanes compared to silica gel (compare BET-measurements), the penetration of the metallocene catalysts into this structure is easily accomplished. This results in the enrichment of the aluminoxane structures that are not directly supported on the carrier surface.

Characterization of the Surface According to the BET Method

According to the SEM recordings, the carrier material–PHT catalyst system exhibits a porous sur-

face independent of the carrier material. A quantitative investigation of the surface area depending on the carrier used was performed with nonhydrolyzed samples under a nitrogen atmosphere. The PHT/carrier systems with silica gel, anhydrous aluminum trifluoride or starch as carriers were investigated as examples. An analysis of the pure, untreated carrier materials without aluminoxane was also conducted. The specific surface area of the catalysts was determined according to the Brunauer, Emmett, and Teller (BET) theory.²⁰ The calculated, relevant data of the investigated samples are summarized in Table II. The pore size was analyzed according to de Boer.

The extreme difference in the surface structure and the pore system of the carrier materials used is indicated clearly by the BET measurement data. Although silica gel exhibits a pore-rich system with a large surface area, starch, and aluminum trifluoride have a surface area that is lower by a factor of 200 and 2000. A completely different picture

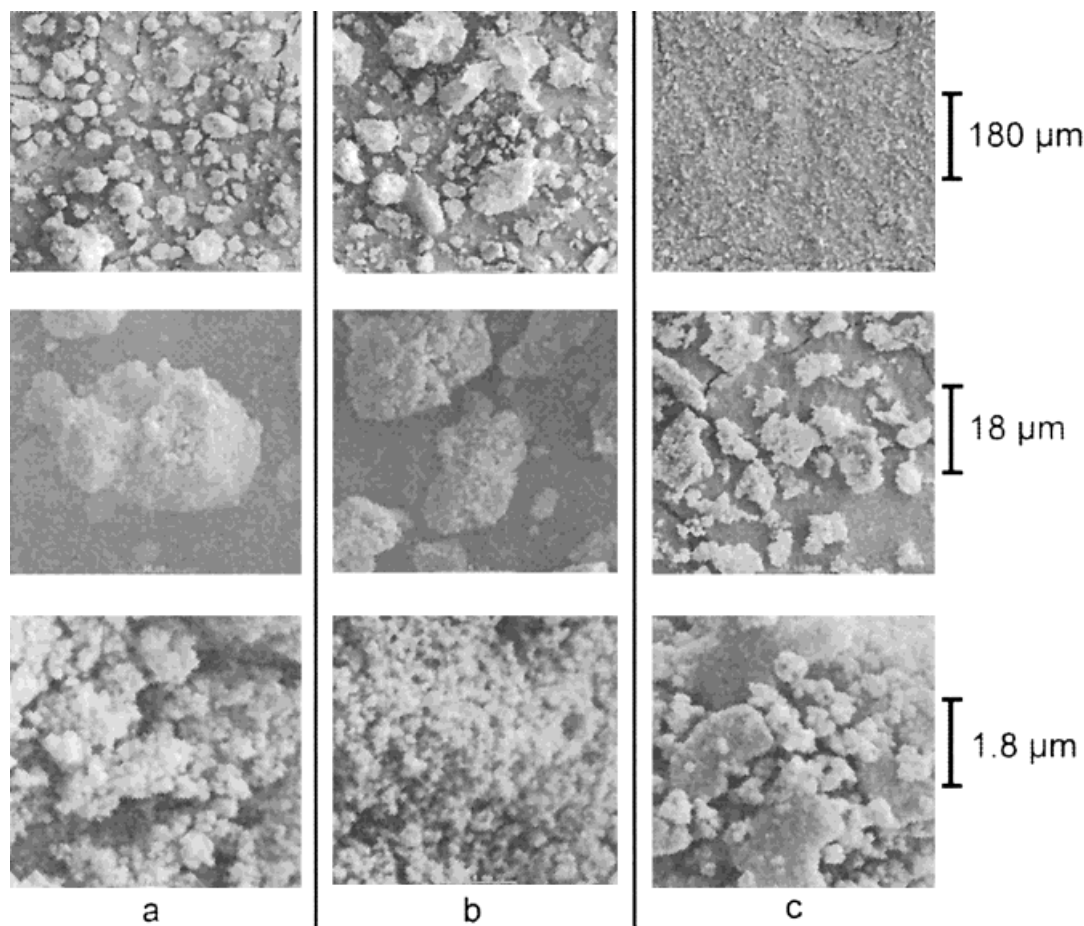


Figure 7 SEM-recording of (a) silica gel-PHT 2, (b) starch-PHT 10, and (c) aluminum-trifluoride-PHT 5.

emerges after supporting the aluminoxane. The surface areas of all three systems are in the range of 60–400 m²/g. The starch system has the largest increase in surface area. This may reflect the fact that it offers ideal anchor points for supporting the smallest aluminoxane spheres due to its amorphous surface covered with hydroxyl groups. The aluminoxane is uniformly distributed over the whole carrier particle. The aluminoxane apparently is formed in the pores of the silica gel as indicated by the much lower pore volumes of the PHT system compared to pure silica gel. Because starch-PHT 10 and silica gel-PHT 2 have almost identical specific surface areas and aluminum trifluoride-PHT 5 possesses only one-sixth of this surface area, a relationship between structure of the carrier material and type and size of the supported aluminoxane spheres is possible. The theory that amorphous carrier materials like silica gel and starch have an irregularly arranged aluminoxane cluster with large surface area (approx. 380 m²/g), is confirmed. The crystal-

line aluminum trifluoride, because of its uniform surface, forces the formation of well-ordered structures of aluminoxane clusters, which results in a small surface area (60.8 m²/g).

FTIR Spectroscopy

Infrared spectroscopic studies on insoluble aluminoxanes are seldom described in the literature.²¹ Based on the results of the solid-state NMR spectroscopic analyses, different molecule vibrations and rotations, which depend on the carrier type used were expected. The infrared spectroscopic characterization of the different cocatalysts made with these carriers, however, are identical and independent of the carrier material. All the IR spectra have identical absorption bands for the aluminoxane portion of the compound. Solvent-free MAO also exhibits wave numbers and signal intensities that are conform with the heterogeneous aluminoxanes. The IR spectra of silica gel-

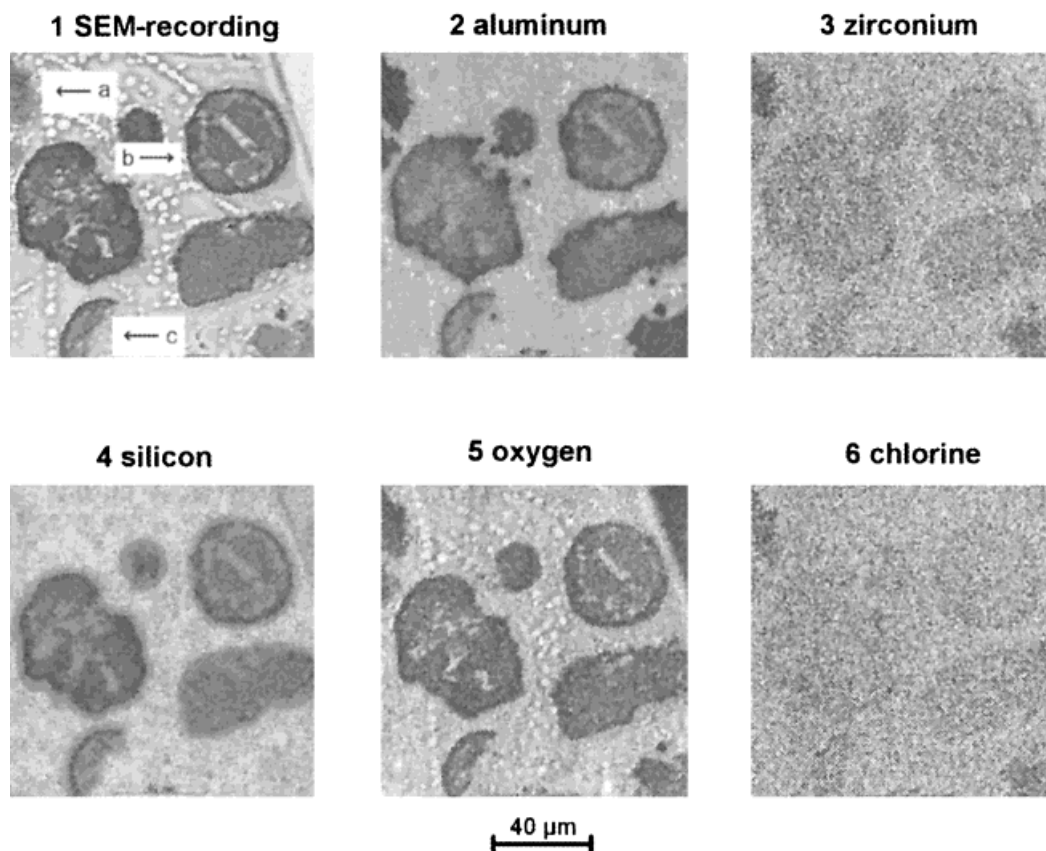


Figure 8 Element specific cross section analyses (2–6) of several silica gel-PHT particles.

PHT 2 (a), starch-PHT 10 (b), and solid MAO (c) are discussed as examples (Fig. 9).

All the synthesized aluminoxanes exhibit four characteristic vibration bands. The C–H stretching vibration of the methyl group on the aluminum atom appears at 2947 cm^{-1} . The relatively broad band at 810 cm^{-1} is assigned to the vibra-

tion of the Al–O–Al unit. The Al–C stretching vibration exhibits a strong absorption band at 700 cm^{-1} . The vibration band at 1218 cm^{-1} is assigned to a C–O stretching vibration. This band appears in all measured samples with similar intensity. This result is consistent with the NMR results, which indicated the presence of methoxy groups. Depending on the carrier used, the vibration bands appear at 470 and 1109 cm^{-1} for the Si–O–Si bending vibration or between 3000 and 3700 cm^{-1} for the O–H valence vibration of the carrier material starch. The results show that in the case of starch, a reaction of the OH groups with TMA occurs only on the surface and that the internal, hydrogen-bonded OH groups are not available for a reaction.

Table II Surface Parameters for the Support Materials and the Combination Support/PHT

Compound	BET Surface (m^2/g)	Pore Volume (cm^3/g)	Average Pore Diameter (\AA)
Silica gel	274.1	1.62	118
Starch	0.155	0.004	473
AlF_3	1,309	0.010	149
Silica gel-PHT ^a	376.5	0.971	51.6
Starch-PHT ^a	384.6	0.664	34.5
AlF_3 -PHT ^a	60.79	0.055	18.0

^a Cocatalyst parameters: Al : Zr = 260 : 1, Al : O = 1.44, aluminoxane portion: 63%.

Polymerization Results

Influence of the Carrier Material:

Table I contains the ethylene polymerization and resin characterization results for the catalysts

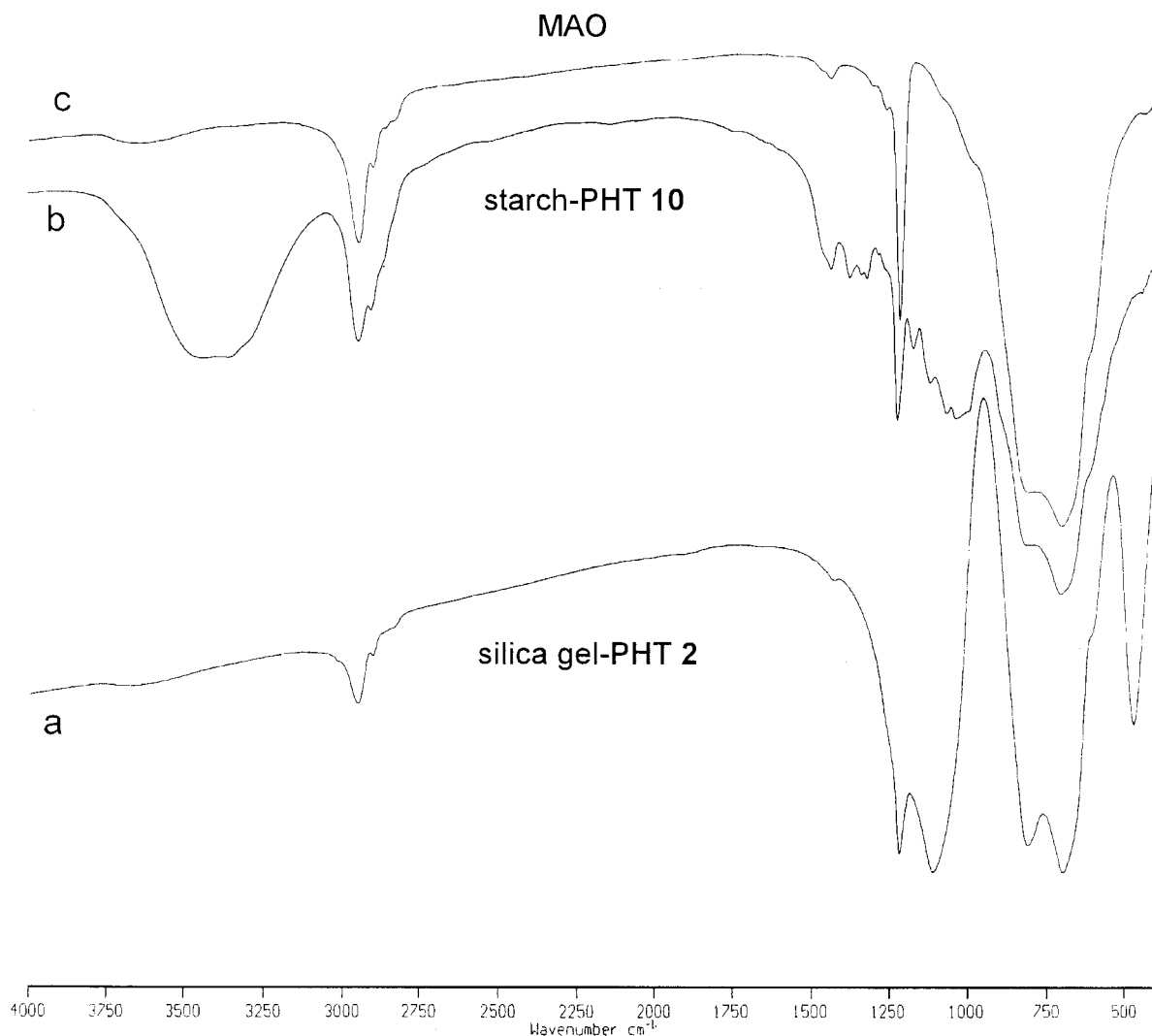


Figure 9 KBr infrared spectra of (a) silica gel-PHT 2, (b) starch-PHT 10, and (c) solid MAO.

with various carrier materials. The high activity maximum obtained for silica gel-PHT 2 compared to the lower values for the other carrier materials is remarkable. The SiO_2 -MAO 1 cocatalyst system known in the literature,¹⁰⁻¹³ where the water required for the aluminoxane synthesis is adsorbed in silica gel, exhibits a significantly lower activity. With the exception of MgCl_2 , none of the carrier materials presented here exhibited a similarly low activity. The synthesis procedures of 1 and 2 were combined to produce catalyst 3, i.e., part of the required amount of water is adsorbed in the silica gel and the other part is added after the reaction with TMA. However, this catalyst, 3, also exhibits a very low activity compared to the other investigated systems.

Nonpolar compounds like aluminum trifluoride are excellently suited as carriers for PHT. This suggests that compounds like polyethylene, polypropylene, polystyrene, or activated carbon should be tried as catalysts. The nonpolar polymers as inert carriers cannot form a coordinated or chemical bond with the strong Lewis acid TMA. With activated carbon a material with a high surface area was used that should lead to an improved activity. Although the anchor points are absent to form a bond with aluminoxane, the four compounds studied are best suited for the new process to synthesize immobilized aluminoxanes.

Only two processes are described in the literature that use starch as a carrier material or additive in Ziegler-Natta polymerization of olefins.

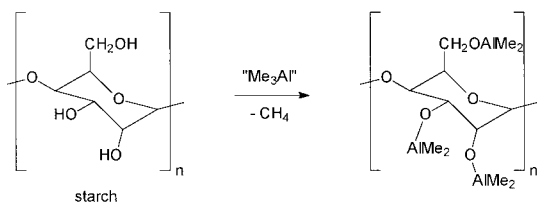


Figure 10 Reaction of starch and trimethylaluminum in toluene.

Kaminsky²² succeeded in activating titanocene dichloride with anhydrous starch after the reaction with TMA. This catalyst system exhibited very low activity (12.5 kg PE/g Ti · h). In the U.S. patent 5,082,882,²³ a process is described where starch is added to a TMA/Ti(OEt)₄ catalyst system as filling material. Catalyst activities of 33.0 kg PE/g Ti · h did not meet the expectations. A similar catalyst system was described by Lee.²⁴ Treating cyclodextrin with MAO or TMA and then reacting it with a metallocene catalyst, produced heterogeneously effective catalyst systems, however, with low activity.

The low activities are a result of the hydroxyl groups, which remain on the polysaccharide surface and cause catalyst poisoning. They react with the activated catalyst center and block it for the polymerization process. MAO, which is relatively inactive compared to TMA, is not able to achieve this.

Starch, cellulose, or commercial flour should be much more effective in the synthesis of immobilized aluminoxanes using the PHT process. All hydroxyl groups on the surface are blocked during the reaction with TMA. Therefore, the catalyst poisoning effect is eliminated. All polyhydroxy compounds used were employed untreated and unmodified for PHT synthesis.

However, the reaction of the hydroxyl groups with TMA is incomplete. Infrared spectroscopic investigations of the activated catalyst samples exhibit a broad band at 3432 cm⁻¹ that is significant for a valence vibration of a bridging hydrogen bond. Consequently, only the surface of the polysaccharide is saturated with aluminoxane groups, the inside of the carrier material remains unchanged.

The aluminum alkyls, chemically bonded on the surface, and free TMA react with steam to form aluminoxane. Cellulose, starch, and flour are excellently suited for immobilization. Obviously, the arrangement of the hydroxyl groups on the surface serves as template for the formation of

aluminoxane structures that exhibit advantageous cocatalyst properties. The activities are in the range of 270 kg PE/g Zr · h, comparable to the activities of the nonpolar polymers like polyethylene-PHT¹⁵ or polypropylene-PHT.¹⁶

If Tylose® (methyl cellulose) is used, no anchor points are available for the formation of an aluminum oxygen bond. The TMA can be supported on the carrier material only by a coordinated bond. Therefore, the arrangement of aluminoxane due to a template effect is not accessible. The consequence is a much lower catalyst productivity (160 kg PE/g Zr · h) compared to cellulose-PHT.¹²

Influence of the Catalyst Precursor

In additional polymerization experiments, the silica gel-PHT cocatalyst system was used with various metallocene catalysts.^{25,26} The results of the polymerization experiments are summarized in Table III. Bis(*n*-butylcyclopentadienyl)zirconium dichloride and 2-(9-fluorenylidene-1-cyclopentadienyldiene)-hex-5-enylidene zirconium dichloride proved to be highly active metallocene catalysts in combination with silica gel-PHT.

Influence of the Aluminum/Zirconium Ratio

The ratio of the catalytically active metal centers to the amount of aluminum in the cocatalyst significantly influences the number of active centers (catalyst activity) as well as the molecular weights of the produced polymers.²⁷ Numerous publications report about the extremely high ratios of aluminum (in MAO) to the transition metal (in the metallocene)^{28,29} that are needed to shift the equilibrium from the inactive metallocene complex Cp₂ZrR₂ or deactivated metallocene species to the catalytically active metallocene catalyst. The catalytic activities drastically decrease for MAO concentrations below an Al : Zr = 300 : 1 molar ratio. Even at an Al : Zr molar ratio above 1000 : 1, the activity increases with the third root of the MAO concentration.³⁰ Bridged bis(flourenyl) complexes of zirconium showed their highest activities with molar aluminum zirconium ratios of 20,000 : 1.³¹

These systems with very high aluminum : zirconium ratios are commercially not applicable, because the required immobilization of the catalyst leads to diffusion problems of the monomer to the catalyst center, which are shielded by an MAO matrix. MAO is relatively expensive due to the costly starting material TMA. Consequently, a 10,000-fold excess of aluminoxane is also not

Table III Polymerization Results^a of Various Catalyst Precursors on SiO₂-PHT

Catalyst Precursor	SiO ₂ -PHT	SiO ₂ -PHT	PE- <i>T</i> _{<i>m</i>,1} (°C),	PE-Δ <i>H</i> _{<i>m</i>,1} (J/g),	PE-α (%)
	Activity (kg PE/g Zr · h)	PE- <i>M</i> _{η (kg/mol)}	<i>T</i> _{<i>m</i>,2} (°C)	Δ <i>H</i> _{<i>m</i>,2} (J/g)	
Cp ₂ ZrCl ₂ , 18	80	245	—, 140.1	—, 155.2	53
(MeCp') ₂ ZrCl ₂ , 19	53	340	107.4, 142.1	3.2, 153.5	52
(ⁿ BuCp') ₂ ZrCl ₂ , 20	532	132	—, 137.1	—, 147.8	50
(Flu'-C(Me)C ₄ H ₇ -Cp')ZrCl ₂ , 21	518	350	—, 139.1	—, 133.9	45
(Flu'-CH ₂ -Cp')ZrCl ₂ , 22	36	460	—, 137.1	—, 154.2	52
(Flu'-C ₂ H ₄ -Cp')ZrCl ₂ , 23	162	350	—, 138.6	—, 177.2	61
(Flu'-C ₂ H ₄ -Flu')ZrCl ₂ , 24	120	415	—, 139.1	—, 165.5	57
(Flu'-SiMe ₂ -Flu')ZrCl ₂ , 25	110	320	—, 140.0	—, 145.4	50

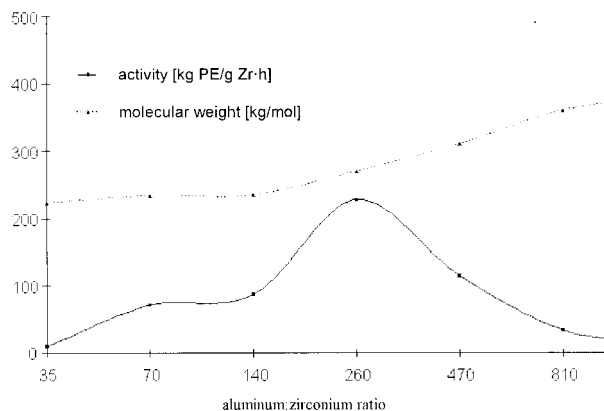
^a Polymerization conditions: 10.0 bar ethylene pressure, 500 mL pentane, 1.0 mL TIBA (1.6 M in *n*-hexane), 70°C, heterogeneous reaction, Al : Zr = 260 : 1, Al : O = 1.44, share of the support SiO₂ in the catalyst: 36%.

Cp' = C₅H₄, Flu' = C₁₃H₈.

feasible due to the cost factor. Therefore, heterogeneous catalyst systems have a significantly lower aluminum : zirconium ratio, and, as a result, they also have considerably lower catalyst activity.

Various aluminoxane systems with controlled zirconium and aluminum concentrations on silica gel were synthesized at an aluminum : oxygen ratio of 1.44 to investigate the influence of the aluminum : zirconium ratio on the catalyst properties of PHT, i.e., the catalyst activity and the polymer properties.

Figure 11 exhibits the effect of various aluminum : zirconium ratios on the catalyst activity and the mean intrinsic viscosity *M*_η of the produced polymer. Maximum catalyst activity is found at a very low aluminum : zirconium ratio of 260 : 1.



Polymerization conditions: 10.0 bar ethylene pressure, 500 ml pentane, 1.0 ml TIBA (1.6 M in *n*-hexane), 70°C, heterogeneous reaction, Al:O = 1.35:1, SiO₂ content of the catalyst: 36%.

Figure 11 Influence of the aluminum : zirconium ratio on catalyst activity and molecular weight of the produced polymers.

The activity decrease at an increased aluminum : zirconium ratio is not very surprising. The space surrounding each Zr center is shielded by a space demanding aluminoxane matrix used to immobilize the catalyst. This creates diffusion problems for the monomer to reach the catalyst center and leads to a slower growth reaction. Therefore, the best loading density on the surface of the catalyst system to obtain a good ion pair separation of the cation and anion is found to be an aluminum : zirconium molar ratio of 260 : 1.

The molecular weight increase at increasing aluminum-zirconium ratios agrees with published data for MAO. These results, obtained from dilution effects favor dissociated, olefin containing ion pairs to their associated precursors and, therefore, increase the chain growth rate compared to the chain termination rate.³²

Polymerization of Propylene:

Surprisingly, the SiO₂/PHT/2 catalyst system with [9-fluorenylidene-1-cyclopentadienyldiene]-2-hex-5-enylidene zirconium dichloride is not suited as a catalyst precursor for syndiotactic propylene polymerization and silica gel/PHT/rac-bis(2-methylindenylidene)dimethylsilylidene zirconium dichloride is not suited for isotactic propylene polymerization. In contrast to the catalyst activated with MAO, the employed catalysts proved to be completely inactive for bulk propylene polymerization at 70°C. An explanation for this unexpected behavior could be the formation of a bulky PHT counter anion in the activation process that blocks monomeric propene to coordinate to the metal.

CONCLUSIONS

PHT makes available a new form of an universally applicable, heterogeneously effective and highly active cocatalyst. It is possible for the first time to support an alumoxane cocatalyst completely on almost any carrier material. The tailoring of cocatalysts with specific properties should be possible by using mixtures of various carrier materials. This approach could allow the production of bi or multimodal resins with only one monomer and one catalyst precursor.

EXPERIMENTAL

Solid-state NMR spectroscopic investigations were performed on a IBM/Bruker WP200 SY spectrometer with a Tecmag Aries control unit and a Chemagnetics MAS measuring head. The samples were filled in 7.5-mm zirconium oxide tubes under inert gas and rotated at a frequency of 7.0 kHz. The ^{13}C NMR measurements (50.32 MHz) were conducted using CPMAS with 2 ms "contact time" and 5 s "delay." Hexamethyl benzene served as external standard. A 1-pulse sequence with a 60° "flip"-angle and 1 s "delay" was used for the ^{27}Al NMR spectra (52.15 MHz). $\text{AlCl}_3 \cdot 6 \text{H}_2\text{O}$ at $\delta = 0$ ppm was used as external reference.

The thermal properties of the polymer samples were investigated for phase transitions using DSC. A NETZSCH DSC 200 instrument was available. For the measurements, 3–6 mg dried polymer were fused into standard aluminum pans ($\phi = 5$ mm) and measured under nitrogen cooling using the following temperature program: first heating phase: from 60 – 200°C , heating rate 20 K/min, isothermal phase (3 min), cooling phase from 200 – 60°C , cooling rate 20 K/min. Second heating phase from 60 – 200°C , heating rate 20 K/min, isothermal phase (3 min), cooling phase from 200 to 20°C , cooling rate 20 °K/min. Melting points and fusion enthalpies were derived from the second heating course. The temperature was linearly corrected relative to indium (m.p. 429.78 °K). The fusion enthalpy of indium ($H_m = 28.45$ J/g) was used for calibration.

The molecular weight determination of the polymer samples was performed using an Ubbelohde precision capillary viscometer in *cis/trans* decalin at $135 (\pm 0.1)^\circ\text{C}$. Therefore, the polymer samples were completely dissolved in decalin at 130°C over a period of 3–4 hs. M_η was determined using calibration curves that were available for three different concentrations.

The aluminoxane catalysts were pressed under inert gas in KBr and measured on air. A FTIR spectrometer Bruker IFS 66v was available.

The SEM recordings were conducted using a JEOL 733 Electron Microprobe. The accelerating potential was 15 kV. The powder samples slowly hydrolyzed in the air and were glued onto electrically conductive, adhesive tape, and subsequently covered with an approx. 300 \AA thick Au/Pd layer. The recordings were digitized with the Software Voyager Version 3.7. For cross-sectional analysis of the particles, the samples were embedded into an epoxy resin, polished, and covered with a thin layer of carbon in a JEOL 4X vacuo evaporator. The recordings were obtained using a NORAN PIONEER spectrometer.

For BET measurements, 0.25 g of the aluminoxane catalyst were filled under inert gas into respective small tubes and dried for 24 *in vacuo* to remove solvent residues. The apparatus used was a Quantachrome Autosorb-6. All measurements were conducted at 77 K.

All the work was routinely carried out with Schlenk technique under strict exclusion of air and moisture. Purified and dried argon was used as inert gas.

Polyolefins as carrier materials: polyethylene (from the homogeneous ethylene polymerization with zirconocene dichloride/MAO (Al : Zr = 1250 : 1), $M_\eta = 310$ kg/mol); polypropylene (isotactic polypropylene from the propylene polymerization with *rac*-bis(2-methylindenylidene)-dimethylsilylidene zirconium dichloride/MAO (Al : Zr = 15000 : 1), $M_\eta = 260$ kg/mol); polystyrene (from the polymerization of cyclopentadienyl titanium trichloride/MAO (Al : Zr = 4000 : 1), $M_w = 20.4$ kg/mol).³³

General Synthesis Procedure for the Carrier Material–PHT Catalyst System

At room temperature, 30 mL of a 2.0 molar trimethylaluminum solution in toluene are added to a suspension of 2.0 g of the carrier material in 100 mL toluene. The subsequent reaction steps are dependent on the carrier material: (a) carrier materials with hydroxyl groups on the surface (starch, flour, cellulose, silica gel): The suspension is heated to 60°C until the gas evolution subsides. Subsequently, the reaction mixture is cooled down to 40°C ; 0.71 mL water is bubbled through the suspension within 15 min using a moist argon flow. (b) Carrier materials without reactive groups on the surface (calcined silica gel, boron

oxide, activated carbon, polyethylene, polypropylene, polystyrene, magnesium chloride, aluminum trifluoride, molecular sieve, tylose®: the suspension is heated to 40°C; 0.75 mL water is bubbled through the suspension within 15 min using a moist argon flow.

Thereupon, the reaction mixture heats itself to 60°C. After 10 min, the suspension becomes suddenly highly viscous. After cooling to room temperature, the mixture is stirred vigorously for 2 h. Finally, the catalyst precursor is added as a solid. The amount is dependent on the desired aluminum : zirconium ratio. Depending on the solubility of the catalyst precursor, the mixture is stirred for 5–30 min. Subsequently, the mixture is filtered and dried *in vacuo*. The filtrate is colorless and contains no organic or inorganic components besides the solvent. Yields of the catalyst: 5.40 g (>95% calculated on the aluminum content) of a powder, colored according to the catalyst precursor.

Synthesis Procedure for the Silica Gel–MAO (1) Catalyst System

Calcined silica gel (2.0 g) (Davison 948) were suspended in 100 mL *n*-pentane and mixed with 0.75 mL water while stirring vigorously. After 30 min, pentane is decanted, and the impregnated silica gel dried for 15 min *in vacuo* without heating.

Thirty milliliters of a 2.0 molar TMA solution in toluene are added to 100 mL toluene at room temperature. Subsequently, the solution is cooled to 10°C and the above impregnated silica gel is added slowly in small portions. After warming the reaction mixture to room temperature it is stirred for 30 min. Finally, 0.23 mmol of the corresponding catalyst precursor is added as a solid, the mixture is stirred for 5 min and filtered. The colored catalyst is dried *in vacuo* for 6 h. The yield of aluminum in aluminoxane is 50%.

We thank Phillips Petroleum Company, Bartlesville, OK, for financial support.

REFERENCES

- Ziegler, K.; Holzkamp, E.; Breil, H.; Martin, H. *Angew Chem* 1955, 67, 541.
- Ziegler, K.; Gellert, H. G.; Zosel, K.; Lehmkuhl, W. *Angew Chem* 1955, 67, 424.
- Natta, G. *Angew Chem* 1956, 68, 393.
- Natta, G.; Pino, P.; Corradini, P.; Danusso, F.; Mantica, E.; Mazzanti, G.; Moraglio, G. *J Am Chem Soc* 1955, 77, 1708.
- Natta, G. *J Polym Sci* 1955, 16, 143.
- Andresen, A.; Cordes, H.-G.; Herwig, J.; Kaminsky, W.; Merck, A.; Mottweiler, R.; Pein, J.; Sinn, H.; Vollmer, H.-J. *Angew Chem* 1976, 88, 689; *Angew Chem Int Ed Engl* 1976, 15, 630.
- Sinn, H.; Kaminsky, W. *Adv Organomet Chem* 1980, 18, 99.
- Sinn, H.; Kaminsky, W.; Vollmer, H.-J.; Woldt, R. BASF AG, U.S. Pat. 4,404,344 (1983).
- Chang, M. Exxon Chemical Co., U.S. Pat. 4,912,075 (1990).
- Schmidt, G. F.; Hucul, D. A.; Campbell, Jr., R. E. Dow Chemical Co., U.S. Pat. 5,015,749 (1991).
- Canich, J. A. M.; Licciardi, G. F. Exxon Chemical Co., U.S. Pat. 5,057,475 (1991).
- Tsutsui, T.; Ueda, T. Mitsui Petrochemical Ind., U.S. Pat. 5,234,878 (1993).
- Chang, M. Exxon Chemical Co., U.S. Pat. 5,529,965 (1996).
- Burkhardt, T. J.; Murata, M.; Brandley, B. W. Exxon Chemical Co., U.S. Pat. 5,240,894 (1993).
- Janiak, C.; Rieger, B. *Angew Macromol Chem* 1994, 215, 47.
- Soga, K.; Arai, T.; Nozawa, H.; Uozumi, T. *Macromol Symp* 1995, 97, 53.
- Sugano, T. *J Mol Catal* 1993, 82, 93.
- Janiak, C.; Rieger, B.; Voelkel, R.; Braun, H.-G. *J Polym Sci Part A Polym Chem* 1993, 31, 2959.
- Peifer, B.; Milius, W.; Alt, H. G. *J Organomet Chem* 1998, 553, 205.
- Lowell, S.; Shields, J. *Powder Surface Area and Porosity*; Chapman and Hall: London, 1984, 2nd ed.
- Tsutsui, T.; Kioka, M.; Toyota, A. Mitsui Petrochem Ind., U.S. Pat. 4,990,640 (1991).
- Kaminsky, W. CPC International Inc., U.S. Pat. 4,431,788 (1984).
- Pettijohn, T. M. Phillips Petroleum Co., U.S. Pat. 5,082,882 (1992).
- Lee, D.; Yoon, K. *Macromol Symp* 1995, 97, 185.
- Palackal, S. J. Dissertation, University of Bayreuth (1991).
- Patsidis, K. Dissertation, University of Bayreuth (1993).
- Han, T. K.; Ko, Y. S.; Park, J. W.; Woo, S. I. *Macromolecules* 1996, 29, 7305.
- Sinn, H.; Kaminsky, W.; Vollmer, H.-J.; Woldt, R. *Angew Chem* 1980, 92, 396; *Angew Chem Int Ed* 1980, 19, 390.
- Kaminsky, W.; Miri, M.; Sinn, H.; Woldt, R. *Makromol Chem Rapid Commun* 1983, 4, 417.
- Fischer, D.; Mülhaupt, R. *Makromol Chem* 1994, 195, 1433.
- Schertl, P.; Alt, H. G. *J Organomet Chem* 1999, 582, 328.
- Schwartz, J.; Labinger, J. A. *Angew Chem* 1976, 88, 402; *Angew Chem Int Ed Engl* 1976, 15, 333.
- Schmid, C. Dissertation, University of Bayreuth (1996).